



HAL
open science

Controlling dispersity in aqueous atom transfer radical polymerization: rapid and quantitative synthesis of one-pot block copolymers

Hyun Suk Wang, Kostas Parkatzidis, Simon Harrisson, Nghia P. Truong,
Athina Anastasaki

► **To cite this version:**

Hyun Suk Wang, Kostas Parkatzidis, Simon Harrisson, Nghia P. Truong, Athina Anastasaki. Controlling dispersity in aqueous atom transfer radical polymerization: rapid and quantitative synthesis of one-pot block copolymers. *Chemical Science*, 2021, 12 (43), pp.14376-14382. 10.1039/d1sc04241f. hal-03832548

HAL Id: hal-03832548

<https://hal.science/hal-03832548>

Submitted on 27 Oct 2022

HAL is a multi-disciplinary open access archive for the deposit and dissemination of scientific research documents, whether they are published or not. The documents may come from teaching and research institutions in France or abroad, or from public or private research centers.

L'archive ouverte pluridisciplinaire **HAL**, est destinée au dépôt et à la diffusion de documents scientifiques de niveau recherche, publiés ou non, émanant des établissements d'enseignement et de recherche français ou étrangers, des laboratoires publics ou privés.



Distributed under a Creative Commons Attribution - NonCommercial - NoDerivatives 4.0 International License

Controlling Dispersity in Aqueous Atom Transfer Radical Polymerization: Rapid and Quantitative Synthesis of One-Pot Block Copolymers

Hyun Suk Wang,^a Kostas Parkatzidis,^a Simon Harrison,^b Nghia P. Truong,^{a*} Athina Anastasaki^{a*}

Received 00th January 20xx,
Accepted 00th January 20xx

DOI: 10.1039/x0xx00000x

The dispersity (\mathcal{D}) of a polymer is a key parameter in material design, and variations in \mathcal{D} can have a strong influence on fundamental polymer properties. Despite its importance, current polymerization strategies to control \mathcal{D} operate exclusively in organic media and are limited by slow polymerization rates, moderate conversions, significant loss of initiator efficiency and lack of dispersity control in block copolymers. Here, we demonstrate a rapid and quantitative method to tailor \mathcal{D} of both homo and block copolymers in aqueous atom transfer radical polymerization. By using excess ligand to regulate the dissociation of bromide ions from the copper deactivator complexes, a wide range of monomodal molecular weight distributions ($1.08 < \mathcal{D} < 1.60$) can be obtained within 10 min while achieving very high monomer conversions (~99%). Despite the high conversions and the broad molecular weight distributions, very high end-group fidelity is maintained as exemplified by the ability to synthesize *in-situ* diblock copolymers with absolute control over the dispersity of either block (e.g. Low \mathcal{D} \rightarrow High \mathcal{D} , High \mathcal{D} \rightarrow High \mathcal{D} , High \mathcal{D} \rightarrow Low \mathcal{D}). The potential of our approach is further highlighted by the synthesis of complex pentablock and decablock copolymers without any need for purification between the iterative block formation steps. Other benefits of our methodology include the possibility to control \mathcal{D} without affecting the M_n , the interesting mechanistic concept that sheds light onto aqueous polymerizations and the capability to operate in the presence of air.

Introduction

Synthetic polymers differ markedly from small molecules and biomacromolecules such as proteins in that they comprise a distribution of molecular weights. Such distribution, commonly quantified by dispersity (\mathcal{D}), significantly influences a material's properties as it determines both the type and degree of inter- and intra-chain interactions of the constituent polymers.^{1, 2} Reversible deactivation radical polymerization, also referred to as controlled radical polymerization,³ has traditionally focused on reducing \mathcal{D} to the minimum, a strategy attributed to “gaining control” of the polymerization via diminishing chain termination and side reactions. As a consequence, high-dispersity polymers have often been considered undesirable and have widely become identified with “dead” polymer chains, i.e. chains that have lost their end-group and cannot undergo further chain-extension. However, in many applications high- \mathcal{D} polymers exhibit advantageous properties over their low- \mathcal{D} counterparts including in melt rheology,⁴ electrospinning⁵, nanoparticle brushes,⁶ and self-

assembly.⁷⁻⁹ In fact, grades of industrially produced HDPE are characterized by their dispersities and have very different applications,¹⁰ suggesting that there is no “ideal” dispersity. In order to expand the potential applications of polymers consisting of variable molecular weight distributions, methodologies that can provide access to a wide range of \mathcal{D} s while exhibiting high end-group fidelity are required.

To this end, various groups have explored different avenues to control polymer \mathcal{D} . At the early stages, molecular weight distributions were tailored by blending pre-synthesized polymer samples (either of low or high \mathcal{D}) of different molecular weights. Junkers' and our group provided further insight by developing predictive frameworks that allowed custom design of molecular weight distributions.¹¹⁻¹⁵ Recently, Fors and coworkers introduced an innovative semi-batch process to tune the dispersity by regulating initiation in nitroxide-mediated,¹⁶ anionic,^{17, 18} and coordination polymerization.¹⁹ In a different approach, Goto and co-workers exploited the addition of a small amount of a co-monomer during the organocatalyzed reversible complexation-mediated polymerization, enabling access to various architectures and \mathcal{D} s.²⁰ Matyjaszewski's and our group were independently able to demonstrate efficient tailoring of dispersity by reducing the catalyst concentration in atom transfer radical polymerization (ATRP).²¹⁻²⁴ Other approaches include the use of photochromic initiators,²⁵ mixtures of RAFT (reversible addition-fragmentation chain

^a Laboratory of Polymeric Materials, Department of Materials, ETH Zurich, Vladimir-Prelog-Weg 5, Zurich, Switzerland. E-mail: nghia.truong@mat.ethz.ch; athina.anastasaki@mat.ethz.ch

^b LCPO, ENSCBP/CNRS/Université de Bordeaux, UMR5629, Pessac, France

^c Electronic Supplementary Information (ESI) available: Experimental procedures, detailed polymerization results, and SEC and NMR data. See

DOI: 10.1039/x0xx00000x

transfer) agents,^{26, 27} flow chemistry,²⁸⁻³⁴ additives,³⁵ and reducing/termination agents.^{36, 37}

However, these methods operate exclusively in organic media and, to date, no strategy has been reported that can control \mathcal{D} in aqueous media. This is a significant omission limiting both the polymer and application scope. This limitation is partly due to additional complications in aqueous polymerizations, especially for ATRP, which cause increased termination events and side reactions in the form of rapid end-group hydrolysis and dissociation of the deactivator.³⁸ Another issue with existing methods is that the \mathcal{D} of diblock copolymers cannot be fully controlled. For instance, in ATRP it is not currently possible to meaningfully increase the dispersity of a diblock copolymer upon chain-extension (i.e. low \mathcal{D} first block \rightarrow high \mathcal{D} diblock). In a similar vein, when employing RAFT, the \mathcal{D} of the diblock depends on the \mathcal{D} of the initial homopolymer and the RAFTend group, and cannot be arbitrarily controlled. The ability to control the \mathcal{D} in both blocks would be highly advantageous and a step forward in the field of controlled radical polymerization. Furthermore, achieving high monomer conversions when targeting polymers of various \mathcal{D} s is very challenging due to increased termination events when monomer concentration is depleted and also because a significant deceleration of the polymerization rate is often observed when synthesizing such materials.³⁹ For the same reason, one-pot (or “*in-situ*”) diblock copolymers with tunable \mathcal{D} have also not been reported. Last but not least, low initiator efficiency is typically observed for

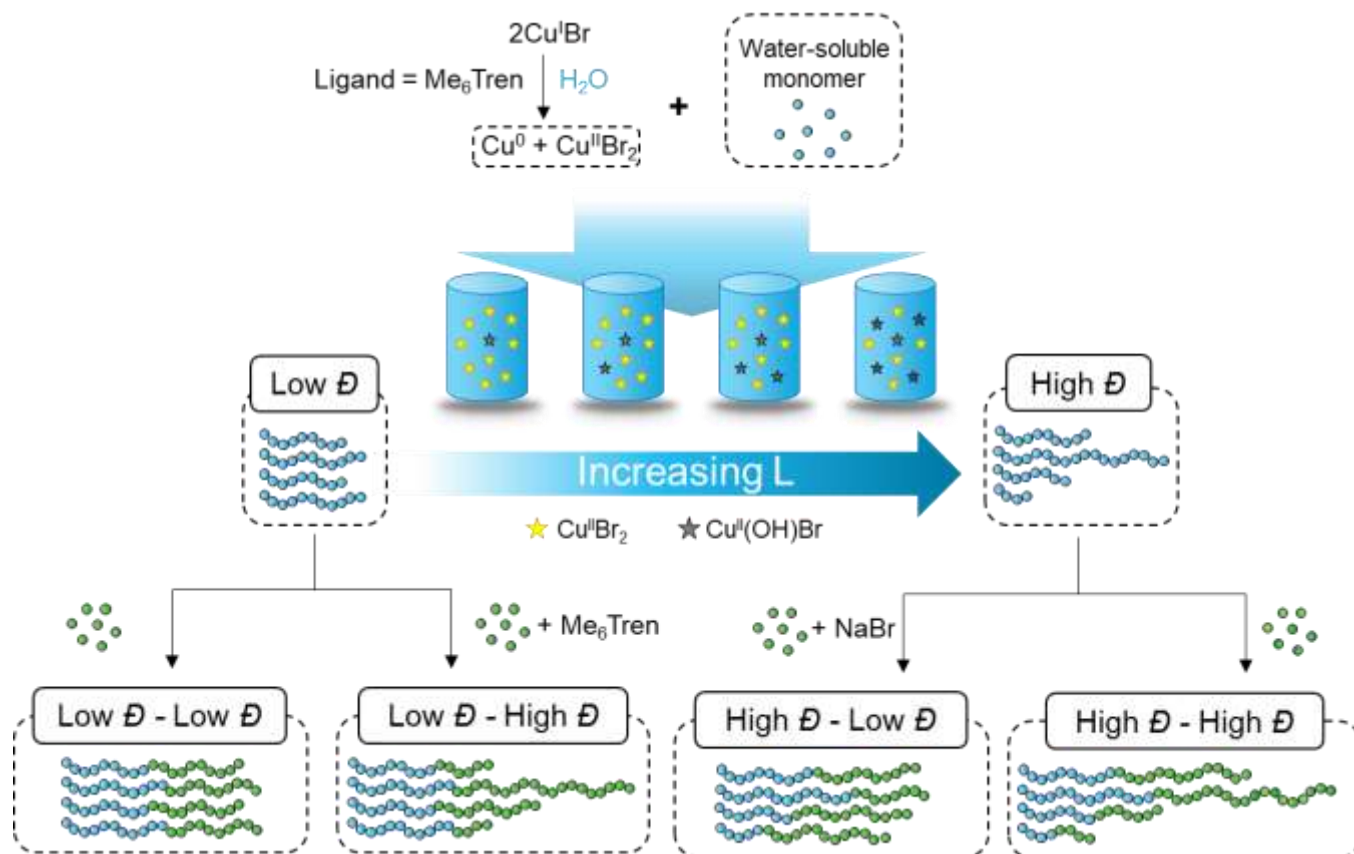
high \mathcal{D} polymers,^{22, 40} thus compromising the efficiency of a given system in block copolymer synthesis.

Results & Discussion

Synthesis of water-soluble polymers with tunable dispersities.

According to the well-established ATRP equation (Eq (1)), lowering the concentration of deactivator can lead to polymers with higher \mathcal{D} s. Thus, the key to successfully controlling polymer \mathcal{D} in ATRP is to determine a way to regulate the deactivator concentration ($[\text{Cu}^{\text{II}}\text{Br}_2]$). In organic media this is possible by directly reducing $[\text{Cu}^{\text{II}}\text{Br}_2]$. However, this is particularly challenging in aqueous media as small amounts of copper deactivator are susceptible to significant halide dissociation.^{41, 42} Hence, our direction was shifted to an alternative method whereby the *in-situ* disproportionation of $\text{Cu}^{\text{I}}\text{Br}$ (yielding Cu^0 and $\text{Cu}^{\text{II}}\text{Br}_2$) is exploited prior to the addition of the initiator and monomer.⁴³ In particular, 2,3-dihydroxypropyl 2-bromo-2-methylpropanoate (GlyBiB) was used as the water-soluble ATRP initiator, tris(dimethylamino)ethyl amine (Me_6Tren) as the ligand and *N*-isopropylacrylamide (NIPAM) as the monomer. The targeted degree of polymerization (DP) was set to 120. 2.4 equivalents of $\text{Cu}^{\text{I}}\text{Br}/\text{Me}_6\text{Tren}$ (with respect to the initiator; $[\text{Cu}^{\text{I}}\text{Br}]:[\text{Me}_6\text{Tren}] = [1]:[1]$) were left to disproportionate in deionized water for 10 min, followed by the addition of an aqueous solution containing the initiator and monomer. Within 10 min, a polymer with fairly low dispersity ($\mathcal{D} \sim 1.15$) was

Scheme 1. Aqueous approach to tailoring the dispersity of water-soluble polymers



obtained at quantitative conversion (>99%) (Table S1, Figure S2). We hypothesized that by reducing the initial [Cu^IBr/Me₆Tren], less [Cu^IBr/Me₆Tren] would be produced from *in-situ* disproportionation, yielding polymers with higher \bar{D} . Indeed, when 0.8 equivalents of [Cu^IBr/Me₆Tren] were employed, a higher \bar{D} was attained ($\bar{D} \sim 1.26$) (Table S1, Figure S4). However, upon further decreasing [Cu^IBr/Me₆Tren] to 0.6 equivalents, a noticeable peak bimodality was observed (Figure S5), and below 0.4 equivalents complete loss of control over polymerization was observed ($\bar{D} \sim 3.5$), indicating insufficient deactivation under the conditions utilized. (Table S1, Figure S6-8). As such, simply lowering [Cu^IBr/Me₆Tren] proved ineffective and a different methodology was required to control polymer dispersity.

$$\bar{D} = 1 + \frac{1}{DP} + \left(\frac{[RBr]_0 k_p}{k_{deact} [[Cu^{II}(L)Br]^+ Br^-]} \right)^2 (q - 1)$$

$$= 1 + \left(\frac{[RBr]_0 k_p}{k_{deact} [[Cu^{II}(L)Br]^+ Br^-]} \right) \text{ when } DP \gg 1 \text{ and } q \approx 1 \quad (1)$$

Instead, we envisioned that to tune polymer \bar{D} , the amount of active copper deactivator complex [Cu^{II}L(Br)]⁺Br⁻ (where L is the ligand Me₆Tren) could be regulated *in-situ* by exploiting its dissociation reaction in aqueous solution. In basic aqueous solution, OH⁻ ions could replace bromide of the active [Cu^{II}L(Br)]⁺Br⁻ deactivator complex, forming an inactive copper complex [Cu^{II}L(OH)]⁺Br⁻. As such, we hypothesized that by modulating the Me₆Tren ligand concentration, which is also a Lewis base that can react with water to produce OH⁻ ions, we could tune the amount of active copper deactivator ([Cu^{II}L(Br)]⁺Br⁻) and ultimately control polymer \bar{D} (see Eq (2)).



To test this hypothesis, the homopolymerization of NIPAM was carried out with a sub-stoichiometric ligand concentration (with respect to Cu^IBr) using the following conditions: [NIPAM] : [Initiator] : [Cu^IBr] : [Me₆Tren] = [120] : [1] : [2.4] : [1.6]. Within 6 min, the complete disappearance of the vinyl signals between 5.5 and 6.5 ppm in the ¹H-NMR spectrum confirmed full monomer conversion (>99%) (Figure S9) and size exclusion chromatography (SEC) showed a symmetrical and monomodal molecular weight distribution with low dispersity ($\bar{D} \sim 1.09$, $M_n \sim 27,700$) (Figure 1a, Table S2). When a ratio of ([Cu^IBr] : [Me₆Tren] = [2.4] : [2.4]) was employed, a polymer with comparable molecular weight could be obtained, albeit with a slightly higher dispersity ($\bar{D} \sim 1.14$, $M_n \sim 28,400$). Following our initial hypothesis, further increase in the ligand concentration ([Cu^IBr] : [Me₆Tren] = [2.4] : [4.8], [2.4] : [6.0], and [2.4] : [7.2]) led to a gradual broadening of the molecular weight distribution, yielding polymers with $\bar{D} \sim 1.33$, 1.40 and 1.60, respectively (Figure 1a, Table S2). Importantly, in all cases, monomodal molecular weight distributions could be maintained without any visible tailing, suggesting negligible termination. In addition, quantitative conversions (>98%) could be achieved within 10 min regardless of the targeted \bar{D} . This is

a significant improvement over previous methods in which moderate conversions (e.g. 16%) and slower rates of polymerization (e.g. 2-5 h) were observed for higher \bar{D} polymers.²² Another major advantage of our strategy is that altering ligand concentration only affects \bar{D} rather than M_n . In previous systems, changing \bar{D} was accompanied by a significant variation in M_n .²² Alternatively, we were able to maintain a constant peak molecular weight M_p (and thereby, also the weight-average molecular weight M_w) as the physical properties of polymeric materials hinge more critically on their M_w rather than M_n . (Figure 1b, Table S3). The latter data also allow for a better visualization of the gradual broadening of the molecular weight distributions.

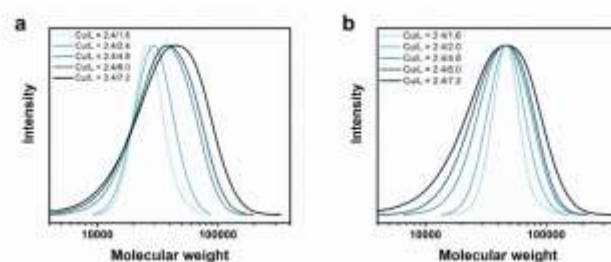


Figure 1. Tuning the dispersity of PNIPAM in water using different [Cu^IBr]:[Me₆Tren] ratios while maintaining constant (a) target DP and (b) M_p .

Unravelling the effect of ligand on the dissociation of Cu^{II}Br₂.

We were also interested in providing a preliminary mechanistic insight to further understand the effectiveness of our methodology. Our initial hypothesis was that the ligand could *in-situ* reduce the concentration of active copper deactivator ([Cu^{II}L(Br)]⁺Br⁻) via the reaction shown in Eq (2), thus producing polymers with higher \bar{D} . If this were the case, and following Eq (2), supplying bromide salts would drive the equilibrium back to the left-hand side and regenerate the deactivator.^{44, 45} To test this, NaBr was added to the polymerization with a threefold excess of ligand ([Cu^IBr] : [Me₆Tren] = [2.4] : [7.2]) which, without the salt, produced high- \bar{D} PNIPAM. Indeed, when 120 eq. NaBr was added, the resulting \bar{D} was 1.12, in stark contrast to reactions without NaBr that possessed a much higher dispersity ($\bar{D} = 1.6$) (Figure S10). This data strongly suggest that dissociation is indeed the driving force behind the increase in \bar{D} . Next, to confirm that Me₆Tren increased halide dissociation by producing hydroxyl ions, various amounts of NaOH were added to reactions with no excess ligand ([Cu^IBr] : [Me₆Tren] = [2.4] : [1.6]), which would also reduce the concentration of active copper deactivator and produce high- \bar{D} PNIPAM (equation 2). In agreement with our hypothesis, increasing the NaOH content did indeed increase \bar{D} as did excess ligands (Figure S11, S12a, Table S4). The relationship between pH and halide dissociation can be qualitatively understood in terms of the generation of the inactive deactivator as shown in Eq (3). Qualitatively, the relationship between Me₆Tren concentration and the ratio of inactive to active copper deactivator can be expressed with Eq

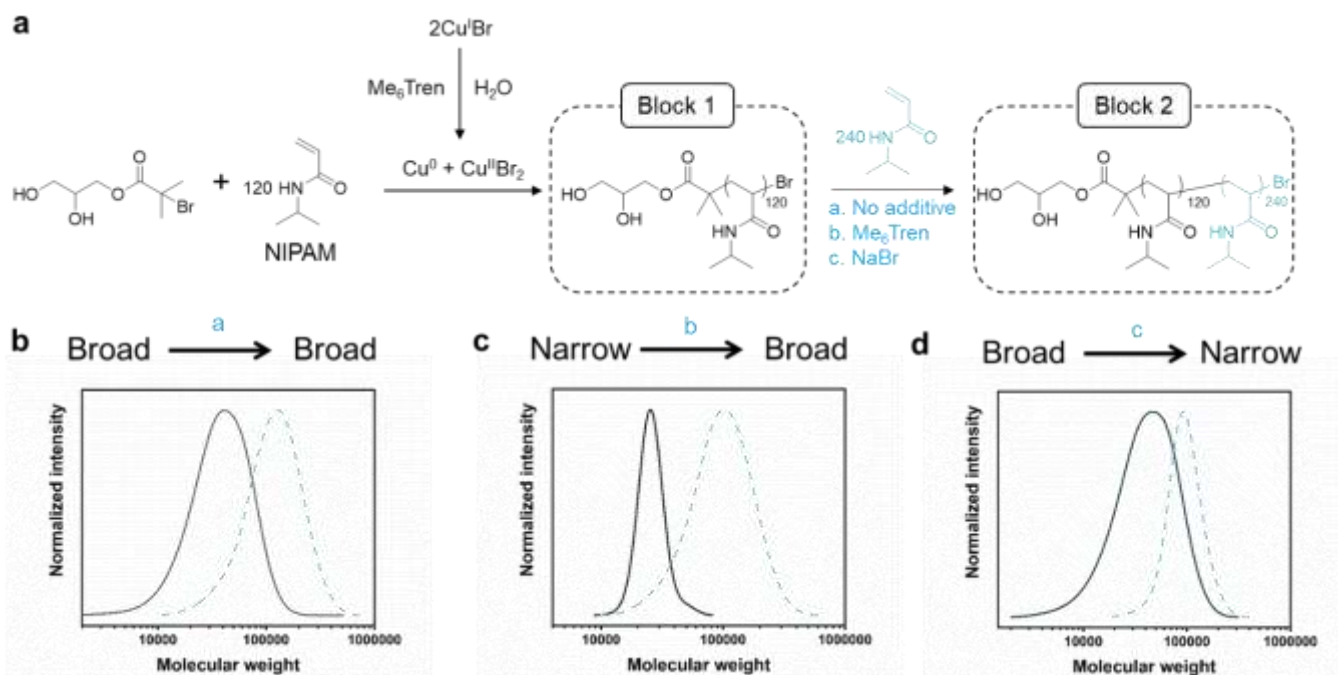
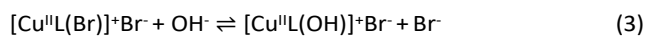


Figure 2. (a) synthesis of one-pot PNIPAM-*b*-PNIPAM with individually tunable blocks via the Cu/L ratio for the first block and either Me₆Tren or NaBr for the second block. (b) SEC traces for high-to-high, (c) low-to-high, and (d) high-to-low dispersity diblocks.

(4), whose derivation can be found in the Supporting Information, where K_b is the base dissociation constant of Me₆Tren and K_d is the halide dissociation equilibrium constant for Eq (2). Although Eq (4) is not derived to quantitatively calculate the dispersity values, it can be seen that increasing ligand concentration increases \bar{D} (Figure S12b) whereas an increase in [Br⁻] (directly correlated to the amount of NaBr added) decreases \bar{D} (Figure S10), in agreement with our experimental results. Finally, Eq (4) can be further applied to the well-established equation for \bar{D} in ATRP to give Eq (S6). To summarize, we concluded that by increasing the ligand concentration, the concentration of the active [Cu^{II}L(Br)]⁺Br⁻ deactivator was (reversibly) reduced through halide dissociation and thereby the rate of deactivation was decreased, ultimately leading to higher \bar{D} s.



$$\bar{D} \sim \frac{\text{inactive deactivator}}{\text{active deactivator}} = \frac{[\text{Cu}^{\text{II}}\text{L}(\text{OH})]^+\text{Br}^-}{[\text{Cu}^{\text{II}}\text{L}(\text{Br})]^+\text{Br}^-} \\ = \frac{K_d(-K_b + \sqrt{K_b^2 + 4[\text{Me}_6\text{Tren}_{\text{added}}]K_b})}{2[\text{Br}^-]} \quad (4)$$

Assessing chain-end fidelity in diblock copolymers with tunable \bar{D} . Dissociation is often considered to be an undesirable side reaction, yielding polymers with poor end-group fidelity. As we were interested in creating living high- \bar{D} polymers, we aimed to explore the livingness of our polymers through the synthesis of a variety of diblock copolymers whereby any \bar{D} combination would be feasible (Figure 2a). In particular, three variations of

chain extensions were designed: high-to-high, low-to-high and high-to-low \bar{D} . In the first example, a high \bar{D} PNIPAM ($\bar{D} \sim 1.5$, DP = 120) was prepared. After reaching full monomer conversion (>99%), a second aliquot of NIPAM was added, yielding a diblock copolymer with $\bar{D} \sim 1.5$ (Figure 2b). It is worth noting that a high DP was targeted for the second block (DP 240) to visualize the clear shift in the SEC trace and thereby demonstrate the living nature of the high- \bar{D} first block. As a demonstration of the versatility in terms of monomer scope, a high-to-high dispersity chain extension was performed with poly(hydroxyethyl acrylamide) (PHEAM) (Figure S13) yielding comparable data. For the low-to-high block copolymer, a sub-stoichiometric amount of Me₆Tren ([Cu^IBr] : [Me₆Tren] = [2.4] : [1.6]) was used for the synthesis of the first block to yield a PNIPAM with $\bar{D} = 1.07$ and subsequently chain-extended with more monomer and an additional amount of Me₆Tren (3.2 eq) to end up with a final \bar{D} of 1.41 (Figure 2c). To the best of our knowledge, this is the first demonstration of a living polymerization methodology that allows such low-to-high transition as previous methodologies – both (semi)batch and continuous systems – have limited control over the dispersity of the second block. Finally, for the high-to-low block copolymer, the first block was synthesized with threefold excess Me₆Tren to Cu^IBr ([Cu^IBr] : [Me₆Tren] = [2.4] : [7.2]) to yield a dispersity of 1.64 and subsequently chain-extended with a monomer solution (DP = 240) containing 120 eq. NaBr to yield quasi-diblock with a final dispersity of 1.17 (Figure 2d). Identical data could also be obtained if instead of NaBr, we inject Cu^{II}Br₂ together with the monomer addition (Figure S14). Importantly, the livingness of this system is especially noteworthy given that a loss of the halogen at the chain end via hydrolysis is a notorious side reaction in water. In summary, these are the first

examples of “*in-situ*” diblocks with full control over the dispersity and extremely high monomer conversions for both blocks (>98%). Simply by adding either Me₆Tren or NaBr (or, alternatively, Cu^IBr₂) to each chain extension, one could control the final \bar{D} regardless of the \bar{D} of the first block.

with chain termination. To this end we attempted to synthesize a high- \bar{D} PNIPAM quasi-hexablock copolymer with a first block of target DP = 120 and the subsequent blocks of DP = 30 (Figure 3). Each chain extension was allowed to proceed for 5-8 min to achieve quantitative conversions (>98%) prior to the

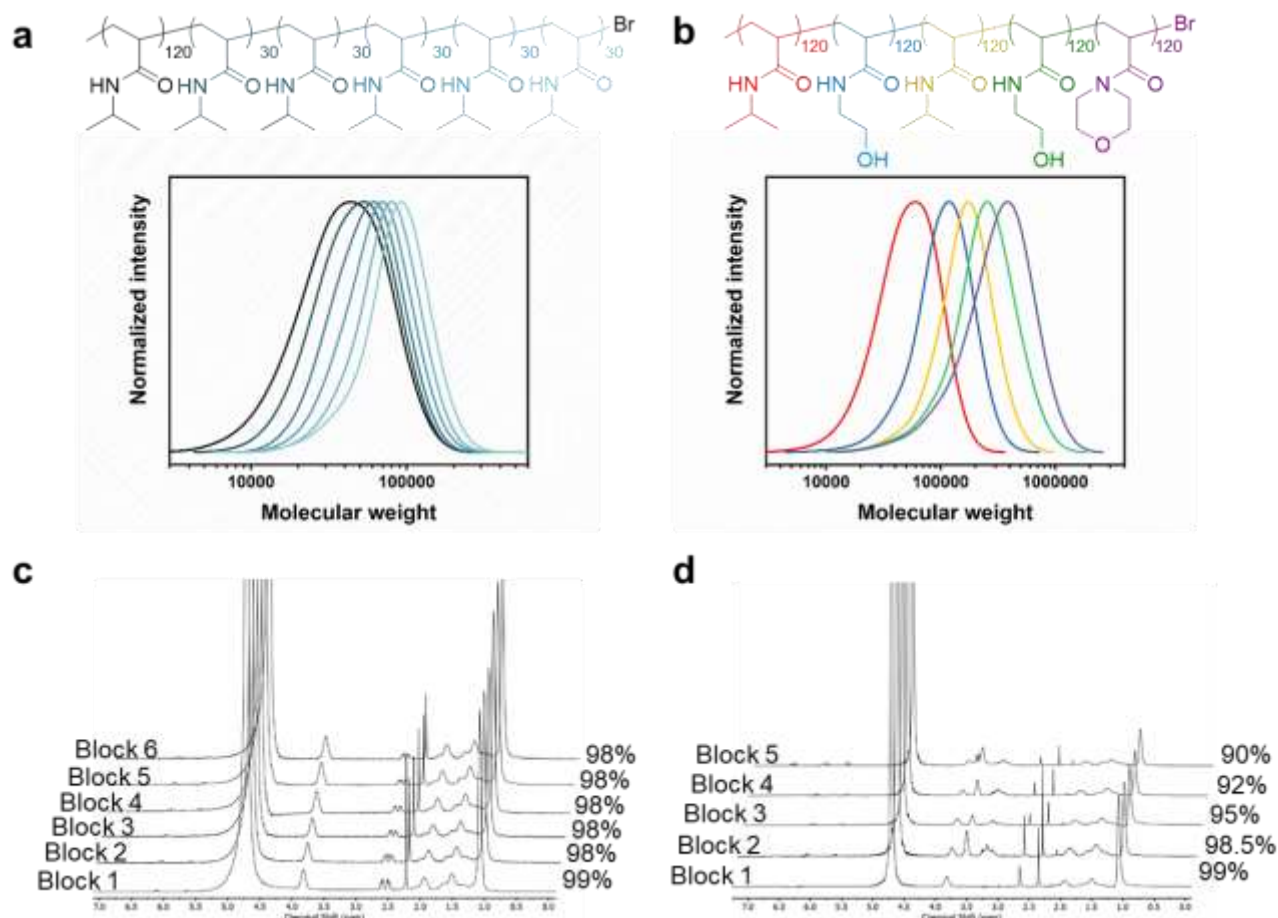


Figure 3. Chemical structure and SEC traces of (a) PNIPAM hexablock and (b) PNIPAM-*b*-PHEAM-*b*-PNIPAM-*b*-PHEAM-*b*-PNAM pentablock. Corresponding NMR spectra of each block in the (c) hexablock and (d) pentablock prior to monomer addition.

Robustness and versatility of the methodology. Considering the high polymerization speed, we were interested in investigating the reproducibility of our method. To achieve this, eight batches of high- \bar{D} PNIPAM were polymerized under the same conditions ($[\text{Cu}^{\text{I}}\text{Br}] : [\text{Me}_6\text{Tren}] = [2.4] : [7.2]$) to quantitative conversion and their SEC traces were overlaid with each other (Figure S15). The deviations between batches were very minor, strongly evidencing the robustness and reproducibility of the methodology, especially since polymerization proceeds to full conversion, circumventing uncertainties regarding the duration of polymerization. In addition, we sought to explore whether we could extend our developed strategy to different monomer classes. Pleasingly, when poly(ethylene glycol) methyl ether acrylate (PEGA) was polymerized with different $[\text{Cu}^{\text{I}}\text{Br}] : [\text{Me}_6\text{Tren}]$ ratios a similar trend was observed, yielding materials with tunable \bar{D} s. (Figure S16-17, Table S5-6). To further probe the potential of our methodology, we were also interested in the limits of livingness for high- \bar{D} systems as high \bar{D} has traditionally been associated

subsequent chain extension (Figure 3c). As seen in Figure 3a, even with a first block of $\bar{D} = 1.55$, there are clear shifts in the SEC trace upon each of the six chain extensions, indicating high retention of the terminal Br. A gradual increase in tailing on the lower molecular weight could be observed when additional chain extensions were attempted yielding a decablock copolymer (Figure S18-19, Table S7). For added chemical intricacy, we attempted to synthesize a challenging high- \bar{D} pentablock copolymer consisting of PNIPAM, PHEAM, and poly(*N*-acryloylmorpholine) (PNAM) with a much higher total molecular weight. A DP of 120 was targeted for each block and clear shifts in the SEC traces despite the high dispersity and aqueous medium evidenced both the livingness of the system and its compatibility with other monomers (Figure 3b). It is worth noting that the final M_n was as high as 221,600 g/mol which represents the highest molecular weight multiblock copolymer targeted to date (Table S8). Moreover, it should be highlighted that such high-order multiblock copolymers can be synthesized in less than one hour for the decablock (~90 min for the higher molecular weight pentablock copolymer) which also

represents a remarkable acceleration in polymerization rate over previous ATRP methods.⁴⁶⁻⁴⁸ Last but not least, well-defined multiblock copolymers could be obtained in the absence of any external deoxygenation (Figure S20, Table S9) thus further highlighting the robustness of our approach and expanding the accessibility of our materials to non-experts.

Conclusions

We introduce the first example of aqueous radical polymerization through which the dispersity can be efficiently tuned while maintaining monomodal molecular weight distributions. The key to our approach is to modulate the reversible dissociation of the bromide ion from copper deactivator by simply varying the ligand concentration, which ultimately determines the concentration of the active deactivator Cu^IBr₂ complex. Unlike previous methodologies, the dispersity could be fully controlled in both homopolymers and diblock copolymers while all reactions reach near-quantitative monomer conversions within 10 min. The very high end-group fidelity attained in our system was further exemplified by the rapid synthesis of *in-situ* multiblock copolymers targeting both lower and higher molecular weight materials in an efficient manner. Both acrylamide- and acrylate-based monomers were compatible with our methodology, and high reproducibility and oxygen-tolerance were also demonstrated. Given the tremendous importance of dispersity across different disciplines in both academia and industry, we envision this work will attract broad interest beyond the field of polymer chemistry.

Author Contributions

A.A. and N.P.T. conceived and designed the research. H.S.W. performed the experiments. K.P. contributed to the experiments. H.S.W., K.P., S.H., N.P.T., A.A. contributed to the analysis of data and co-wrote the manuscript.

Conflicts of interest

There are no conflicts to declare.

Acknowledgements

A.A. gratefully acknowledges ETH Zurich for financial support. N.P.T. acknowledges the award of a DECRA Fellowship from the ARC (DE180100076). This project has received funding from the European Research Council (ERC) under the European Union's Horizon 2020 research and innovation programme (DEPO: grant agreement No. 949219).

Notes and references

1. V. A. H. Boudara, J. D. Peterson, L. G. Leal and D. J. Read, *J. Rheol.*, 2019, **63**, 71.
2. C. Tsenoglou, *Macromolecules*, 1991, **24**, 1762.
3. K. Parkatzidis, H. S. Wang, N. P. Truong and A. J. C. Anastasaki, *Chem*, 2020, **6**, 1575.
4. M. Collis and M. Mackley, *J. Non-Newtonian Fluid Mech.*, 2005, **128**, 29.
5. L. Palangetic, N. K. Reddy, S. Srinivasan, R. E. Cohen, G. H. McKinley and C. Clasen, *Polymer*, 2014, **55**, 4920.
6. S. J. Park, S. Kim, D. Yong, Y. Choe, J. Bang and J. U. Kim, *Soft Matter*, 2018, **14**, 1026.
7. D. T. Gentekos and B. P. Fors, *ACS Macro Lett.*, 2018, **7**, 677.
8. D. T. Gentekos, J. Jia, E. S. Tirado, K. P. Barteau, D.-M. Smilgies, R. A. DiStasio Jr and B. P. Fors, *J. Amer. Chem. Soc.*, 2018, **140**, 4639.
9. I. Kim and S. Li, *Polym. Rev.*, 2019, **59**, 561.
10. M. P. McDaniel and P. J. DesLauriers, in *Kirk-Othmer Encyclopedia of Chemical Technology*, 2000, pp. 1.
11. T. Junkers and J. H. Vrijnsen, *Eur. Polym. J.*, 2020, **134**, 109834.
12. J. H. Vrijnsen, M. Rubens and T. Junkers, *Polym. Chem.*, 2020, **11**, 6463.
13. M. Rubens and T. Junkers, *Polym. Chem.*, 2019, **10**, 5721.
14. T. Junkers, *Macromol. Chem. Phys.*, 2020, **221**, 2000234.
15. R. Whitfield, N. Truong and A. Anastasaki, *Angew. Chem. Int. Ed.*, 2021, DOI: <https://doi.org/10.1002/anie.202106729>.
16. D. T. Gentekos, L. N. Dupuis and B. P. Fors, *J. Amer. Chem. Soc.*, 2016, **138**, 1848.
17. V. Kottisch, D. T. Gentekos and B. P. Fors, *ACS Macro Lett.*, 2016, **5**, 796.
18. S. Domanskyi, D. T. Gentekos, V. Privman and B. P. Fors, *Polym. Chem.*, 2020, **11**, 326.
19. R. J. Sifri, O. Padilla-Vélez, G. W. Coates and B. P. Fors, *J. Amer. Chem. Soc.*, 2020, **142**, 1443.
20. X. Liu, C. G. Wang and A. Goto, *Angew. Chem. Int. Ed.*, 2019, **131**, 5598.
21. A. Plichta, M. Zhong, W. Li, A. M. Elsen and K. Matyjaszewski, *Macromol. Chem. Phys.*, 2012, **213**, 2659.
22. R. Whitfield, K. Parkatzidis, M. Rolland, N. P. Truong and A. Anastasaki, *Angew. Chem. Int. Ed.*, 2019, **58**, 13323.
23. Z. Wang, J. Yan, T. Liu, Q. Wei, S. Li, M. Olszewski, J. Wu, J. Sobieski, M. Fantin and M. R. Bockstaller, *ACS Macro Lett.*, 2019, **8**, 859.
24. M. Rolland, V. Lohmann, R. Whitfield, N. P. Truong and A. Anastasaki, *J. Polym. Sci.*, DOI: <https://doi.org/10.1002/pol.20210319>.
25. D. Liu, A. D. Sponza, D. Yang and M. Chiu, *Angew. Chem. Int. Ed.*, 2019, **58**, 16210.
26. K. Parkatzidis, N. P. Truong, M. N. Antonopoulou, R. Whitfield, D. Konkolewicz and A. Anastasaki, *Polym. Chem.*, 2020, **11**, 4968.
27. R. Whitfield, K. Parkatzidis, N. P. Truong, T. Junkers and A. Anastasaki, *Chem*, 2020, **6**, 1340.
28. M. Rubens and T. Junkers, *Polym. Chem.*, 2019, **10**, 6315.
29. D. J. Walsh, D. A. Schinski, R. A. Schneider and D. Guironnet, *Nat. Commun.*, 2020, **11**, 3094.
30. N. Corrigan, A. Almasri, W. Taillades, J. Xu and C. Boyer, *Macromolecules*, 2017, **50**, 8438.
31. N. Corrigan, R. Manahan, Z. T. Lew, J. Yeow, J. Xu and C. Boyer, *Macromolecules*, 2018, **51**, 4553.
32. J. Morsbach, A. H. E. Müller, E. Berger-Nicoletti and H. Frey, *Macromolecules*, 2016, **49**, 5043.
33. M. H. Reis, T. P. Varner and F. A. Leibfarth, *Macromolecules*, 2019, **52**, 3551.

34. K. Liu, N. Corrigan, A. Postma, G. Moad and C. Boyer, *Macromolecules*, 2020, **53**, 8867.
35. C.-G. Wang, A. M. L. Chong and A. Goto, *ACS Macro Lett.*, 2021, **10**, 584.
36. V. Yadav, N. Hashmi, W. Ding, T.-H. Li, M. K. Mahanthappa, J. C. Conrad and M. L. Robertson, *Polym. Chem.*, 2018, **9**, 4332.
37. K.-I. Seno, S. Kanaoka and S. Aoshima, *J. Polym. Sci. Pol. Chem.*, 2008, **46**, 2212.
38. M. Teodorescu and K. Matyjaszewski, *Macromolecules*, 1999, **32**, 4826.
39. A. Goto and T. Fukuda, *Prog. Polym. Sci.*, 2004, **29**, 329.
40. M. Rolland, N. P. Truong, R. Whitfield and A. J. A. M. L. Anastasaki, *ACS Macro Lett.*, 2020, **9**, 459.
41. N. V. Tsarevsky, T. Pintauer and K. Matyjaszewski, *Macromolecules*, 2004, **37**, 9768.
42. M. Fantin, A. A. Isse, A. Gennaro and K. Matyjaszewski, *Macromolecules*, 2015, **48**, 6862.
43. Q. Zhang, P. Wilson, Z. Li, R. McHale, J. Godfrey, A. Anastasaki, C. Waldron and D. M. Haddleton, *J. Amer. Chem. Soc.*, 2013, **135**, 7355.
44. X. Pan, N. Malhotra, A. Simakova, Z. Wang, D. Konkolewicz and K. Matyjaszewski, *J. Amer. Chem. Soc.*, 2015, **137**, 15430.
45. A. Simakova, S. E. Averick, D. Konkolewicz and K. Matyjaszewski, *Macromolecules*, 2012, **45**, 6371.
46. A. Anastasaki, V. Nikolaou, G. S. Pappas, Q. Zhang, C. Wan, P. Wilson, T. P. Davis, M. R. Whittaker and D. M. Haddleton, *Chem. Sci.*, 2014, **5**, 3536.
47. A. H. Soeriyadi, C. Boyer, F. Nyström, P. B. Zetterlund and M. R. Whittaker, *J. Amer. Chem. Soc.*, 2011, **133**, 11128.
48. A. Anastasaki, C. Waldron, P. Wilson, C. Boyer, P. B. Zetterlund, M. R. Whittaker and D. Haddleton, *ACS Macro Lett.*, 2013, **2**, 896.